International Journal of Applied Glass Science 1–11 (2012)
DOI:10.1111/ijag.12003

INTERNATIONAL JOURNAL OF
Applied Glass
SCIENCE

Structure of Rhenium-Containing Sodium Borosilicate Glass

Ashutosh Goel,* John S. McCloy,† Charles F. Windisch Jr, Brian J. Riley, Michael J. Schweiger, and Carmen P. Rodriguez,

Pacific Northwest National Laboratory, Richland, Washington 99352

José M.F. Ferreira

Department of Ceramics and Glass Engineering, University of Aveiro, CICECO 3810-193, Aveiro, Portugal

A series of sodium borosilicate glasses were synthesized with $KReO_4$ or Re_2O_7, to 10,000 ppm (1 mass%) target Re, to assess effects of large concentrations of rhenium on glass structure and fto estimate solubility of ^{99}Tc, a radioactive component in low active waste nuclear glasses. Rhenium was used as a surrogate for ^{99}Tc for laboratory testing, due to similarities in chemistry, ionic size, and redox. Magic angle spinning nuclear magnetic resonance, Fourier transform infrared spectroscopy, and Raman spectroscopy were performed to characterize the glasses. Si was coordinated in Q^2 and Q^3 units, Al was four-coordinated, and B was mostly three-coordinated. The rhenium additions did not have significant effects on the glass structure up to approximately 3000 ppm Re by mass, the maximum concentration that remained dissolved in glass. Rhenium likely exists in isolated ReO_4^- anions in the interstices of the glass network, as evidenced by polarized Raman spectrum of the Re glass in the absence of sulfate. Analogous to SO_4^{2-} in similar glasses, ReO_4^- is a network modifier and above solubility forms alkali salt phases on the surface and in the bulk. Comparisons of phase separation and crystallization in MoO_4^{2-} containing borosilicate glasses can also be made to ReO_4^- containing glasses.

Introduction

Roughly 200,000 m^3 of high-level waste is currently stored in 177 underground tanks at the Hanford site near Richland, Washington. This waste was generated by the reprocessing of roughly 100,000 t of spent uranium fuel to recover materials for defense purposes. The initial part of reprocessing comprised of chemical decladding of the fuel (primarily aluminum clad fuel was processed, but also some zirconium clad and steel clad fuels) using three primary processes: (i) bismuth phosphate carrier precipitation, (ii) REDOX solvent extraction, and (iii) PUREX solvent extraction. In each

*Present address: Sterlite Technologies Ltd. E-1, E-2, E-3, MIDC Waluj Aurangabad Maharashtra 431136 India
†john.mccloy@pnnl.gov

case, the fuels were chemically declad leading to the generation of radioactive wastes. Further, the generated wastes were primarily neutralized with NaOH and stored in carbon steel tanks. Once in the tanks, some wastes were further processed to remove water, uranium, cesium, and strontium. The combination of these processes generated a highly complex waste stream that is not found anywhere else in the world.

The cornerstone of Hanford tank waste management strategy is the Hanford tank waste treatment and immobilization plant (WTP), which is currently under construction and is expected to begin operation within this decade. The WTP will receive the waste from tanks and separate it into high-level waste (HLW) and low-activity waste (LAW) fractions by the following series of processes: (i) the HLW solids will be filtered and washed to remove excess supernatant, (ii) aluminum and chromium will be removed by caustic and oxidative leaching (respectively), (iii) the cesium will be removed from the liquid fraction by ion exchange, and finally (iv) excess water will be removed from the LAW fraction by evaporation. The resulting LAW fraction that contains <5% of the activity and >90% of the mass and volume will be treated separately from the HLW fraction. The currently designed WTP will vitrify all the HLW and roughly 30% of the LAW fractions of the tank waste. The additional 70% of the LAW will be treated by a yet-to-be-determined process for onsite waste disposal.

Technetium and Rhenium

Technetium (from Greek τεχνικός, meaning artificial) is a fission product of uranium[1] and therefore is present in nuclear waste including Hanford tank waste. Technetium is known to be predominantly in the pertechnetate form in most of the Hanford tank waste and is expected to partition to the LAW fraction when processed through WTP as described above. ^{99}Tc is a radioactive isotope of particular concern due to its very high mobility in ground water (as pertechnetate ion, TcO_4^-) and long half-life (2.1×10^5 years). The primary concern in processing the waste containing ^{99}Tc is its volatility and hence low retention in a glass waste form processed by melting.[2] Volatility is not problematic in evaporation and drying processes but does creates trouble in high temperature molten glass processing from either liquid or dried feed.[2] Other sources of ^{99}Tc loss could include entrainment with volatilized solvent, formation of aerosols, dust particles in scrubber systems, and other similar sources, which can be partially mitigated by engineering systems and recycling.[3] Some recent work has looked at the relative importance of volatility with and without the cold cap.[4] Partitioning to the molten salt phase has also been suggested as a mechanism for low retention of Re (^{99}Tc) in glass.[5] Volatilization can occur from the salt layer more readily than from the glass, especially if sulfate is present.[6]

Rhenium has been used as a surrogate material for ^{99}Tc for laboratory testing, as its chemistry, ionic size, and other chemical aspects are very similar, more so than other candidates such as Mn, W, or Ru.[3] Rhenium commonly occurs in the 7+ oxidation state as Re_2O_7 or ReO_4^- (perrhenate ion), but also in the 4+ state in ReO_2 and the 6+ state in ReO_3 (unlike ^{99}Tc).[3,7,8] Studies of Re diffusion heated in air (oxidizing conditions) have shown that Re^{7+} in a glass melt is reduced to Re^{6+} near the surface of the melt to oxidize Fe^{2+} to Fe^{3+} in a coupled redox reaction, with Re^{6+} species diffusing faster than Re^{7+} species.[7] In hydrothermal fluids, Re is predicted to be present with Cl in a Re^{4+} oxidation state.[7] In silicate melts of the diopside-anorthite eutectic (Si–Al–Ca–Mg–O), Re is present as Re^{6+} and Re^{4+} with no evidence for Re^{7+} even at high oxygen fugacities (fO_2).[9] Rhenium compounds should be similar to those expected for technetium in LAW simulants ($KReO_4$), and in liquid ($CsReO_4$, $NaReO_4$, and $KReO_4$) and vapor (Re_2O_7 and $ReO_3(OH)$) phases during vitrification.[3]

Some significant differences in behavior between Re and ^{99}Tc in glass are important to consider. A key difference between ^{99}Tc and Re is that Tc^{7+} is more easily reduced to Tc^{4+} than is Re^{7+} to Re^{4+}.[3,10] In experiments with glasses of varying redox conditions comparing ^{99}Tc to Re, only Re^0 and Re^{7+} but no Re^{4+} or Re^{6+} were observed, even though in comparable ^{99}Tc glasses Tc^0, Tc^{4+}, and Tc^{7+} were observed.[11] Thus, it has been suggested that, at least in borosilicate LAW glasses, Re may not be a representative substitute for ^{99}Tc under reducing conditions.[11] Additionally, in vapor hydration tests (VHTs[12]), ^{99}Tc was always reduced to Tc^{4+} regardless of the starting distributions of ^{99}Tc valence, whereas Re^{7+} species were always dominant in the comparable Re glasses.[10,13] While ^{99}Tc is enriched at the outer corroded gel layer of amorphous silicate and almost absent at the center, Re concentrations are low near the surface of comparable samples and approach that of unreacted glass near the center.

This result highlights the different mobility of Re and ^{99}Tc in hydrothermal environments. However, it should be noted that the corrosion mechanism in VHT tests is not representative of that expected for waste glass in a disposal environment, particularly with regard to temperature.[14] Additionally, a series of recent melter tests suggest that the retention of Re is approximately 8% higher than ^{99}Tc for similar glasses.[4]

Recently, the authors have reported that the solubility of Re as Re^{7+} in sodium borosilicate glass is approximately 3000 parts per million (ppm) by mass.[15,16] Additionally, it was shown that above this limit, rhenium forms surface salt phases and alkali perrhenate crystals in the glass.[16] The current paper focuses on the characterization of the glass structure of rhenium-containing sodium borosilicate glasses using magic angle spinning nuclear magnetic resonance (MAS-NMR), Fourier transform infrared (FTIR) spectroscopy, and Raman spectroscopy.

Glass Selection

Composition of the AN-105 waste simulant (expressed in oxides and halides, shown in Table I) was used for designing the glass for this study.[17] This waste simulant was chosen for its low concentration of SO_3. Sulfate was previously identified as an important consideration for ^{99}Tc retention during the feed melt process, since pertechnetates (and perrhenates) will partition to the low-melting salt phases, which may interfere with Re/^{99}Tc solubility tests. The study glass was initially designed following the current LAW glass formulation rules established for the Hanford waste treatment & immobilization plant (WTP).[18] This glass is similar to the LAWE4H glass used as a baseline case for ^{99}Tc retention studies, which was also formulated based on an old AN-105 waste simulant (previous estimate of AN-105 LAW composition).[4] The as-formulated glass was modified by removing Cl and F to reduce complications with the formation of volatile ^{99}Tc/Re halides as it is known that halides of pertechnetate (e.g., TcO_3Cl, TcO_3F) are highly volatile.[3,19] The final Re study glass composition along with the compositions of as-formulated and LAWE4H glasses are shown in Table I. It should be noted that a small amount of K_2O is already present in this formulation while an additional amount of potassium is incorporated in glasses where $KReO_4$ is used as a rhenium precursor.

Experimental

Glass Synthesis

Rhenium-containing glasses were heated in vacuum-sealed (approximately 10^{-4} Pa, approximately 10^{-6} Torr) fused quartz ampoules so that any Re species in the gaseous phase would still remain in contact with the glass melt surface. This special configuration was designed to determine the solubility of rhenium in this glass, as discussed elsewhere.[15,16] This glass-making process is uncommon for oxide glass synthesis, but has been used for synthesis of iodine-containing glass,[20,21] and is routinely used for processing nonoxide glasses.

The "baseline" sodium borosilicate LAW glass composition was shown in Table I. This glass was synthesized by melt quenching from oxides (MgO, Al_2O_3, SiO_2, Cr_2O_3, ZrO_2, TiO_2, ZnO, Fe_2O_3), carbonates ($CaCO_3$, Na_2CO_3, K_2CO_3), H_3BO_3, and Na_2SO_4. The glass batch was homogenized, melted in a platinum alloy crucible at 1200°C for 1 h, and quenched on a steel plate. This glass was then crushed inside a tungsten carbide mill within a vibratory mixer to yield a fine glass powder "frit."

Target concentrations of Re added to the baseline glass were 0, 100, 1000, 2500, 4000, 6407, 6415, and 10,000 ppm, defined as parts per million, by mass, of Re atoms in the glass. The rhenium source was $KReO_4$ (Alfa Aesar, 99% metal basis, Re 64 mass%). In one experiment, Re_2O_7 (NOAH Tech., 99.99%, −4 mesh) was used as an alternative Re source to assess the influence of different Re precursors (with the same oxidation state) on the Re solubility in glass under a controlled environment. Fractions of the other components in the glasses with Re additions were kept in constant ratios with those in the baseline glass, renormalized to the remaining mass fraction after accounting for the Re source chemical.

Two additional glasses were prepared without sulfur, one with and one without rhenium. The composition was chosen such that the relative molar amounts of all the components were the same as the baseline glass minus the SO_3, and the composition was renormalized. To this "sulfate-free baseline" glass was added 6415 ppm Re (by mass) as $KReO_4$.

Each batch of glass powder (frit + Re source) was placed into a fused quartz tube, and a fused quartz end cap was inserted into the tube.[16] The tube was then evacuated to approximately 10^{-4} Pa and sealed with an

Table I. Glass Composition (in Mass%) for Initial Re Study

Oxide	AN-105 LAW (%)	WTP rules, formulated glass (%)	Re study glass (%)	LAWE4H glass (%)
Al_2O_3	17.99	6.10	6.10	5.97
B_2O_3	0.08	10.00	10.00	9.79
CaO	0.00	2.07	2.07	2.46
Cl	2.18	0.593*	0.00	0.20
Cr_2O_3	0.07	0.02	0.02	0.08
F	0.01	0.003*	0.00	0.08
Fe_2O_3	0.00	5.50	5.50	5.38
K_2O	1.73	0.47	0.47	0.54
MgO	0.00	1.48	1.48	1.45
Na_2O	77.25	21.00	21.00	21.27
NiO	0.00	0.00	0.00	0.01
P_2O_5	0.00	0.00	0.00	0.12
PbO	0.00	0.00	0.00	0.01
SiO_2	0.10	44.71	45.30	44.49
SO_3	0.59	0.16	0.16	0.41
TiO_2	0.00	1.40	1.40	1.37
ZnO	0.00	3.50	3.50	3.43
ZrO_2	0.00	3.00	3.00	2.94
SUM	100.00	100.00	100.00	100.00
			WL = 27.2%†	WL = 27.7%†

AN-105 LAW: simulated low-sulfur low-activity waste (LAW) used in recent glass formulation studies for the Office of River Protection (ORP),[17] which is one of the initial LAW streams to be processed at WTP.
WTP rules, formulated glass: formulated following the current WTP glass formulation rules.
Re study glass: Cl and F (total 0.596 mass%) were deleted and replaced by SiO_2.
LAWE4H glass: Vitreous State Laboratory glass comparable to Re study glass but formulated with previous assessment of AN-105, thus composition differences in NiO, PbO, P_2O_5, and SO_3. This glass included for comparison because Tc retention tests have been performed on it.[4]
*Deleted components from WTP formulation, sum = 0.596%.
†Waste loading (WL) in mass%, based on AN-105 LAW.

oxygen–propane torch. This vacuum-sealed ampoule was inserted in the furnace preheated to 700°C. Subsequently, the temperature increased from 700°C to 1000°C at 5°C/min, followed by a dwell of 2 h at 1000°C to ensure the homogenization of the glass. At the end of the heating time, the ampoule containing the glass melt was quenched in air within a stainless steel canister. Further details on the processing can be found elsewhere.[15]

Magic Angle Spinning Nuclear Magnetic Resonance Spectroscopy

Magic angle spinning nuclear magnetic resonance (MAS-NMR) spectroscopy was performed on a subset of the glasses to investigate the Si, Al, and B structure of the glasses. The ^{29}Si MAS-NMR spectra were recorded on a Bruker ASX 400 spectrometer operating at 79.52 MHz (9.4 T) with a 7-mm probe at a spinning rate of 5 kHz. The pulse length was 2 μs with a 60 s delay time, and kaolinite was used as the chemical shift reference. The ^{27}Al MAS-NMR spectra were recorded at 104.28 MHz (9.4 T) with a 4-mm probe at a spinning rate of 15 kHz. The pulse length was 0.6 μs with a 4 s delay time, and $Al(NO_3)_3$ was used as the chemical shift reference. The ^{11}B MAS-NMR spectra were recorded at 128.36 MHz (9.4 T) with a 4-mm probe at a spinning rate of 12 kHz. The pulse length was 3.6 μs with a 2 s delay time, and H_3BO_3 was used as the chemical shift reference.

Fourier Transform Infrared Spectroscopy

Infrared spectra of the glasses were obtained using a Fourier transform infrared (FTIR) spectrometer (Mattson Galaxy S-7000, Madison, Wl). For this

purpose, glass powders were mixed with KBr in the proportion of 1/150 (by mass) and pressed into a pellet using a hand press. For both the background and sample collection, 64 scans were co-added with a signal gain of 1 at a 4 cm^{-1} resolution.

Raman Spectroscopy

Raman spectra were acquired from bulk glass samples in a backscattering configuration with a Spex (Edison, NJ) Model 1877 Raman spectrometer equipped with Princeton Instruments (Trenton, NJ) liquid-nitrogen-cooled charge-coupled device detector. The 488.0-nm line of a Coherent (Santa Clara, CA) Innova 307 Ar^+ ion laser was used for excitation. The slit width was 400 μm and the exposure time was 15 s for most samples (100 s for the samples without sulfate). Spectral acquisition and data analysis were performed using Princeton Instruments Winspec software and Thermo Fisher Scientific (West Palm Beach, FL) Grams/32AI software, respectively. The estimated uncertainty of the peak frequencies is ± 1 cm^{-1}.

On a limited number of glasses, the plane-polarized (HH or VV) and cross-polarized (HV or VH) Raman spectra were obtained in the 300–1500 cm^{-1} range, where HH indicates that the scattered light was analyzed for an electric vector parallel to that of the incident radiation (i.e., *h*orizontal transmitting, *h*orizontal receiving) and HV indicates that the analysis of the scattered electric vector was perpendicular to that of the incident laser beam (i.e., *h*orizontal transmitting, *v*ertical receiving). Whether the plane polarized was measured as HH or VV, or the cross-polarized was measured as HV or VH, did not significantly affect the results, so these are denoted as "plane," "cross," or "unpolarized."

Results and Discussion

Visual Observations

The following is a brief account of visual observations of the various experiments during quenching, noting particular evidence of volatility, molten salt phases, or other relevant details.

0 ppm Re: During melting and cooling, the surface of the glass and the ampoule stayed clear of any secondary phases. A dimple, approximately 1 cm deep formed in the center of the glass as it solidified. As the glass cooled the ampoule and glass cracked, and later the glass shattered into many small pieces most likely due to stresses from thermal expansion mismatch.

100–4000 ppm Re: The surface of the glass and ampoule stayed clear of any secondary phases. The dimple formed during solidification. Small bubbles formed around the glass surface and the ampoule (like a ring). The ampoule cracked but the glass remained intact.

6400–10,000 ppm Re: As the glass cooled, a separate liquid phase was observed with very low viscosity (<0.1 Pa s) moving on melt surface. This liquid remained on the surface long after the glass became solid but eventually solidified to a white phase. The ampoule did not break, and the glass sample remained as single cylindrical piece with a dimple in the middle of the top surface.

Magic Angle Spinning Nuclear Magnetic Resonance Spectroscopy

Figure 1 presents the MAS-NMR spectra of the investigated glasses for ^{29}Si (Fig. 1a), ^{11}B (Fig. 1b), and ^{27}Al (Fig. 1c) nuclei. The broad ^{29}Si spectra of all the glasses imply a wide distribution of Q^n units or the *degree of polymerization* in the glass structure, where Q denotes the central Si atom and n denotes the number of bridging oxygens around that Si. The ^{27}Al NMR spectra of the glasses manifest signal broadening from paramagnetic-driven relaxation processes and depict the dominance of tetrahedrally coordinated aluminum with its maxima at approximately 56 ppm. We could not confirm the presence of $^{[5]}Al$ and $^{[6]}Al$ species in these glasses with maxima at approximately 30 ppm and 0 ppm, respectively. (Note that the numbers in brackets before the element denote the coordination number of that species, for example, $^{[5]}Al$ denotes 5-coordinated Al.) In particular, the presence of $^{[5]}Al$ species cannot be neglected in these glasses as this species has been reported to exist in a variety of alkali/alkaline earth aluminosilicate glasses.[22] In general, in the presence of high-field strength network modifiers (typically, trivalent ions), significant amounts of AlO_5 and AlO_6 polyhedra may be present in the network, even if charge balancing of all the tetrahedral units is formally possible.[23] Similar complications of coexisting $^{[4]}Al$, $^{[5]}Al$, and $^{[6]}Al$ coordination exist for (Al-B)- or (Al-P)-containing glasses,[24,25] unless Si is present and constitutes the dominating network former (as for the glasses analyzed herein). The $^{[4]}Al$ resonance in all the glasses

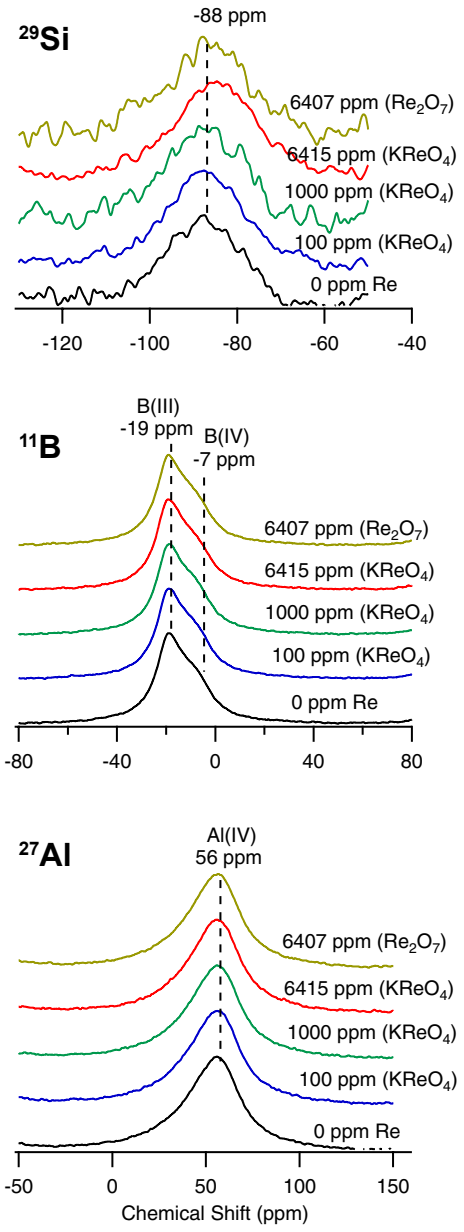

Fig. 1. Magic angle spinning nuclear magnetic resonance curves for Si, B, and Al.

has typical asymmetric forms with tails extending toward lower frequency resulting from the distributions in quadrupolar coupling constants.

With respect to silicon coordination in glasses, the predominant feature that determines a first approximation of the isotropic ^{29}Si chemical shifts is the number of Si and Al atoms attached to the SiO_4 unit being considered in solid aluminosilicates with increasing polymerization of Q^n building units, that is, shielding of the central Si atom increases in the sequence $Q^0 < Q^1 < Q^2 < Q^3 < Q^4$.[26] According to Murdoch *et al.*,[27] an increase in the number of Al next-nearest neighbors de-shields the Si nucleus, on average, by 5.5 ppm/Al neighbor. Also, the presence of several distinct modifier ions and, particularly, additional network formers results in featureless ^{29}Si MAS-NMR spectra, due to the dependence of the ^{29}Si chemical shift on the precise nature and spatial position of other cations and neighboring oxygen species.[23]

A more fundamental problem, however, is the presence of oxides of paramagnetic ions (Fe^{3+}, Cr^{3+}) in the studied glasses. Concentrations of paramagnetic ions in excess of approximately 0.5 mass% are sufficient to produce noticeably broadened NMR signals.[28] Each one of these hurdles severely precludes the quantitative determination of speciation of network formers in these multicomponent nuclear waste glasses. The ^{29}Si peak position for the investigated glasses lies at approximately −88 ppm. A peak position in this range may represent highly polymerized species with many Al neighbors or less polymerized units with low or no Al neighbors. In the present scenario, the latter option with less polymerized silicate units (a mixture of $Q^2 + Q^3$ units) and low or no Al neighbors seems to be more feasible because of high alkali and alkaline earth content in glasses in comparison with Al_2O_3. As mentioned above, the field strength of the modifier cation plays a key role in deciding the aluminosilicate glass structure as the extent of deviation from Al avoidance, and thus, configurational entropy, increases with increasing cation field strength.[29]

The ^{11}B NMR spectra of the various samples reveal two distinct NMR resonances. First is a primary broad peak at −19 ppm, which is typical for less symmetric planar $^{[3]}$B coordinations, and second is a significantly broader shoulder at −7 ppm, assigned to $^{[4]}$B coordination. It should be noted that the effect on the ^{29}Si chemical shift from boron substitutions is not well established and generally depends on boron coordination.[30] With this in mind, $^{[3]}$B are reported to produce insignificant ^{29}Si NMR peak displacements, whereas the formation of Si–O–$^{[4]}$B motifs is predicted to give similar, albeit smaller, changes in the ^{29}Si chemical shift as those to $^{[4]}$Al (due to the higher electronegativity of B compared with Al). High-field ^{11}B NMR studies are required to determine the quantitative values of $^{[3]}$B/$^{[4]}$B. Overall, the MAS-

NMR data suggest that all the glasses have Si, Al, and some B in tetrahedral coordination, along with the majority of B in trigonal coordination. No trends could be assessed with additions of Re up to 6415 ppm.

Fourier Transform Infrared Spectroscopy

The room-temperature FTIR transmittance spectra of the investigated glasses exhibited four broad transmittance bands in the region 300–1500 cm^{-1} (Fig. 2). This lack of sharp features is indicative of the general disorder in the silicate network mainly due to a wide distribution of Q^n units occurring in these glasses. The most intense transmittance bands lie in the 800–1300 cm^{-1} region, the next one between 300–600 cm^{-1} and 1300–1500 cm^{-1} regions, while the least intensive lies in the 650–800 cm^{-1} region.

The broad band in the 800–1300 cm^{-1} region is assigned to the stretching vibrations of the SiO_4 tetrahedron with different numbers of bridging oxygen atoms. In the present case, this band is centered at approximately 985 cm^{-1} suggesting a mixture of Q^2 (Si) and Q^3 (Si) units in the silicate glass network. Further, the bands in the 300–600 cm^{-1} region are due to bending vibrations of the Si–O–Si and Si–O–Al linkages while the bands in the 650–800 cm^{-1} region are related to the stretching vibrations of the Al–O bonds for the $^{[4]}$Al species. Also, the bands at approximately 1420 cm^{-1} correspond to the predominant presence of boron in trigonal coordination in glasses. As the band for boron in tetragonal coordination is overlapped by the broad silicate band in the 800–1300 cm^{-1} region, the presence of boron in tetragonal coordination cannot be neglected. In summary, any structural changes induced by rhenium incorporation in these glasses could not be ascertained by FTIR.

Raman Spectroscopy

Raman spectra of the white salts on the surface of cooled glasses with 6407 ppm (Re_2O_7) and 10,000 ppm rhenium concentrations exhibited sharp and intense bands at approximately 330 cm^{-1} approximately 370 cm^{-1}, 880–890 cm^{-1}, 920–925 cm^{-1}, and 955–960 cm^{-1} (as shown in Fig. 3) confirming the presence of crystalline $NaReO_4$. These phases were also confirmed with X-ray diffraction.[15,16] These Raman bands are typical for different vibrational modes of Re in tetrahedral site symmetry of scheelite ($CaWO_4$) crystal structure.[31,32] The band at approximately 960 cm^{-1} corresponds to a totally symmetric stretch, a pure bending mode at approximately 330 cm^{-1}, an asymmetric stretch at approximately 920 cm^{-1}, and a combined bending and stretching mode at approximately 370 cm^{-1}. The band at approximately 885–890 cm^{-1} represents the internal mode for Re in tetragonal coordination. The remaining characteristic peaks for $NaReO_4$ were not observed due to the spectral range of the instrument, are usually centered at approximately 149 cm^{-1} and 181 cm^{-1}, and correspond to a rotational and translational lattice mode, respectively.[33]

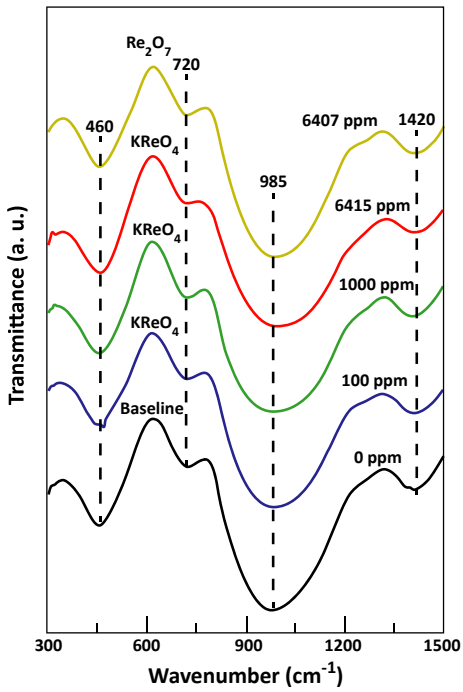

Fig. 2. Fourier transform infrared transmittance spectra of selected glasses.

All of the glass spectra exhibited broad bands in the region of 300–1500 cm^{-1} typical for borosilicate glasses (Fig. 3). No sharp or intense band could be observed in any of the investigated glasses, thus depicting the absence of crystallinity. This observation is in contradiction with XRD results of the 10,000 ppm Re glass, reported previously,[15,16] which showed some weak peaks in the glass due to alkali perrhenate phases. This discrepancy may be attributed to the heterogeneous distribution and low content of crystalline inclusions in the glass matrix as evidenced by laser-ablation inductively coupled plasma-mass spectrometry and elec-

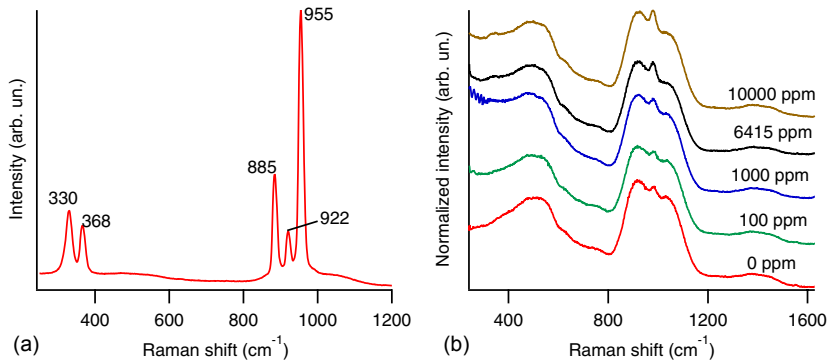

Fig. 3. Raman spectroscopy of (a) $NaReO_4$ white powdered salt from the surface of the Re_2O_7 glass and (b) selected glasses produced with target parts per million (ppm) Re as stated using a $KReO_4$ source; spectra offset for clarity

tron microprobe.[16] Furthermore, in addition to the typical bands for a borosilicate glass composition, a narrow but intense band was observed in all the glasses at approximately 980 cm^{-1} (Fig. 3) denoting the presence of sulfur in these glasses.

The broad band in the 800–1200 cm^{-1} region is assigned to the stretching vibrations of the SiO_4 tetrahedron with different numbers of bridging oxygen atoms. In the preliminary assessment of these glasses with FTIR spectroscopy, the absorption band is centered at approximately 985 cm^{-1} suggesting a mixture of Q^2 and Q^3 units in the silicate glass network. Again, no trends in structural changes of the glass network induced by rhenium incorporation could be assessed with Raman spectroscopy.

The Raman spectra of sulfur containing (Na, Ca)-silicate and borosilicate glasses have a narrow peak near 990 cm^{-1} that is similar in frequency and relative intensity to the symmetric S–O stretch mode of the tetrahedral SO_4^{2-} (sulfate) ions found in aqueous solution, as well as in sodium and calcium sulfate crystals.[34] This primary sulfate Raman peak intensity in glass spectra has been shown to vary almost linearly with respect to sulfur content in glass.[35,36] An additional sulfate peak near 630 cm^{-1}, analogous to that observed for crystalline sulfates, is found in the spectra of glasses with higher sulfur concentrations.[37] Additional peaks in the glasses from the current study were not observed probably due to low sulfur content.

The possibility that sulfide species are present in the investigated glasses is low due to the high fO_2 in the quartz ampoule during glass melting (due to reduction of Fe_2O_3 to FeO) but still its presence cannot be neglected.[36] Therefore, to detect the presence of any other sulfur-containing species in the glasses, polarized Raman spectra were acquired on the glass with Re concentration 6407 ppm (Re_2O_7 source) as presented in Fig. 4a. The polarized Raman measurements demonstrate that the 972 cm^{-1} band in the spectrum of glasses arises from a totally symmetric vibration, that is, symmetric stretch of SO_4^{2-}. As totally symmetric vibrations are strongly polarized, these bands show a marked decrease in the intensity for cross-polarized versus plane-polarized conditions. No other sulfur-containing species could be detected through Raman spectroscopy.

It has been shown by McKeown *et al.*[38] that Raman spectroscopy of borosilicate glasses can clearly exhibit specific modes of Tc^{7+} in fourfold coordination down to concentrations of 50 ppm, but that it is completely insensitive to Tc^{4+} present as $^{[6]}Tc$. However, due to the sulfate band at 980–990 cm^{-1} in the present samples, the weak Raman band for Re^{7+} was not seen, as it should be about the same wavenumber as sulfate (D. A. McKeown, personal communication). The ^{99}Tc band, on the other hand, is sufficiently lower in frequency, at 915 cm^{-1},[38] so as to make it likely visible in the presence of sulfate.

To test this assumption, four glasses were compared with polarized Raman: glasses containing (i) S and Re, (ii) S without Re, (iii) Re without S, and (iv) no S or Re. The results indicate that there is an additional polarized band due to ReO_4^- approximately 970 cm^{-1} that is present in the Re-containing, no-sulfate glass (Fig. 4c), which is not present in the glass with no Re and no S (Fig. 4d). The fact that the perrhenate mode is very near the frequency of the sulfate mode (shown for glasses containing sulfate but no Re in Fig. 4b) illustrates a difficulty in using this band to determine the rhenium

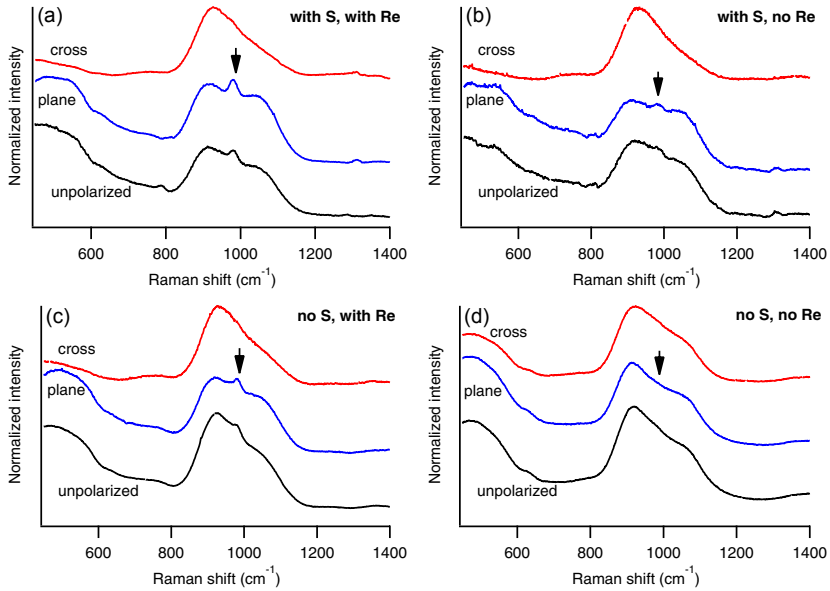

Fig. 4. Unpolarized and (plane- or cross-) polarized Raman spectra with arrow showing peak consisting of sulfate and/or perrhenate vibration for (a) glass with sulfate and 6407 ppm target Re (Re_2O_7 source), (b) glass with sulfate but no Re, (c) glass with no sulfate and 6415 ppm target Re ($KReO_4$ source), and (d) glass with no sulfate and no rhenium. Spectra are offset for clarity.

concentration in the presence of sulfate. This mode, whether sulfate or perrhenate, is not Raman active in the cross-polarized case, suggesting a totally symmetric vibration for perrhenate as well as for sulfate.

X-ray Absorption Near Edge Spectroscopy (XANES) of these samples indicates that in all cases the Re is present Re^{7+} (presented in our earlier work).[15,16] At concentrations up to the solubility approximately 3000 ppm by mass, Re does not appear to affect the overall glass network, as evidenced by negligible differences in the glass Raman spectra, NMR, and FTIR as Re content was increased. Based on the vibrational modes of Re species as determined from Raman spectroscopy, Re is posited to exist in the network as isolated ReO_4^- anions. Additional support for this is provided by the fact that the fundamental Raman vibration for tetrahedral ReO_4 in the glass (990 cm^{-1}, from the current work) is in the same range as ReO_4^- ions in sodalite crystals (975 cm^{-1})[31] in water (971 cm^{-1})[39] and in crystalline $NaReO_4$ (955 cm^{-1}, from the current work).

Comparison of Perrhenate, Sulfate, and Molybdate in Borosilicate Glass

There are several notable similarities between the behavior of sulfate and perrhenate in sodium borosilicate glasses. In analogy to SO_4^{2-}, ReO_4^- should act as a network modifier in the glass, but the soluble concentration of ReO_4^- in these glasses is insufficient to detect changes in the glass structure in the presence of a much higher concentration of glass modifiers (i.e., alkali). In Mishra *et al.*,[40] 1 mol% SO_4^{2-} corresponded to approximately 15°C decrease in the glass transition temperature, but at 2 mol% SO_4^{2-}, structural change was only barely detectable by Si and B NMR. As the solubility of ReO_4^- in the sodium borosilicate LAW glass is approximately 0.1 mol% ReO_4^-, it is unlikely to show measurable effects on glass structure as seen by NMR or Raman spectroscopy. XANES of sulfate-containing glasses indicates that SO_4^{2-} is present as a free ion as well and not bonded to the silicate network.[41] Also, the behavior of sulfate above solubility is similar to perrhenate. At high concentrations of SO_4^{2-}, alkali (Na_2SO_4) or alkaline earth ($BaSO_4$) sulfate salts will form as inclusions in the glass or at salt layers,[40] analogous to the formation of (Na, K)ReO_4 salts in the rhenium-containing glasses.

There are also similarities between the behavior of perrhenate and molybdate in borosilicate glass. In French (SON68) and UK nuclear waste glasses, which contain significant fractions of molybdenum, a salt phase can form as well. This water-soluble phase can

contain radionuclides such as $^{137}Cs/^{135}Cs$ and ^{90}Sr, which can be partitioned to the molten molybdate/chromate/sulfate/chloride salt ("yellow phase").[40,42–44] Extended X-ray absorption fine structure spectroscopy (EXAFS) has suggested that Mo in borosilicate glass forms MoO_4^{2-} tetrahedra that are unconnected with the borosilicate network but rather associated with alkali and alkaline earth regions.[45] Others have suggested that MoO_3, at least at increasing concentrations, acts as a "reticulating agent" for the silicate network where Q^4 units are increased, and the molybdate exists in a "depolymerized region" rich in alkali and alkaline earth ions and nonbridging oxygens.[46,47] However, this situation is related in a complex way to the $^{[3]}B/^{[4]}B$ ratio through the distribution of Na as a charge compensator.[46] Similarly to the cases of sulfate and perrhenate, molybdate in glass eventually forms precipitates of Na_2MoO_4 or other alkali molybdates or $CaMoO_4$. Molybdenum is known as a nucleating agent or crystallization catalyst for glass–ceramics, and its nucleating role is believed to be due to its location in the glass surrounded by alkali and alkaline earths and disconnected from the network.[45]

It is not immediately clear from the current data on ReO_4^- in glass whether ReO_4^- is present as isolated tetrahedra in the glass, surrounded by alkali and alkaline earths, or as bands of tetrahedra in an overall depolymerized region. From the molybdate data, it appears that these two possibilities may be concentration and also glass composition dependent. In either case, the result is the same, in that the metal-oxygen tetrahedra come in close proximity with alkali or alkaline earth ions, are weakly associated with the glass network, and thus tend to phase separate and crystallize. Future work should involve comparing solubility and structural incorporation of TcO_4^-, ReO_4^-, SO_4^{2-}, MoO_4^{2-}, and CrO_4^- in borosilicate glass, since these likely all tend to associate into a low-melting, water-soluble salt phase and concentrate radioactive components such as ^{99}Tc, $^{137}Cs/^{135}Cs$, and halides.

Conclusions

Magic angle spinning nuclear magnetic resonance (MAS-NMR), Fourier transform infrared (FTIR) spectroscopy, and Raman spectroscopy were conducted to characterize glasses as a function of Re source additions. In general, these techniques showed a glass composed of primarily Q^2 and Q^3 structural units, with Si, Al, or B tetrahedra, due to the large sodium content causing nonbridging oxygens. Aluminum was found to be four-coordinated, and boron was largely three-coordinated with some four-coordinated. Rhenium source additions did not appear to have clear effects on the glass structure as evidenced by MAS-NMR, FTIR, and Raman spectroscopy, and there was no discernible difference in effects between $KReO_4$ and Re_2O_7 glasses with the same fraction of Re. Thus, at the concentrations that remain in glass, approximately 3000 ppm Re by mass maximum, the Re does not have a strong effect on the glass structure. Rhenium likely exists in isolated ReO_4^- anions in the interstices of the glass network, as evidenced by the polarized Raman spectrum of the Re glass without sulfate. Many analogies can be drawn between perrhenate and sulfate behavior in sodium borosilicate glasses. Technetium analogues (TcO_4^-) in glass, where ^{99}Tc is Tc^{7+}, should be expected to behave similarly to ReO_4^- and SO_4^{2-}.

Acknowledgments

This work was supported by the Department of Energy's Waste Treatment & Immobilization Plant Federal Project Engineering Division under the direction of Dr. Albert A. Kruger. The authors thank Dr. Dong-Sang Kim and two anonymous reviewers for their valuable comments on the paper. Thanks to Dr. John Vienna for providing the background context for the Hanford site. Pacific Northwest National Laboratory is operated by Battelle Memorial Institute for the U.S. Department of Energy under contract DE-AC05-76RL01830.

References

1. N. N. Greenwood and A. Earnshaw, "Manganese, Technetium and Rhenium," *Chemistry of the Elements*. Butterworth Heinemann, Oxford, 1040–1069, 1997.
2. H. Lammertz, E. Merz, and S. Halaszovich, "Technetium Volatilization During HLLW Vitrification," *Mat. Res. Soc. Symp. Proc.*, 44 823–829 (1985).
3. J. G. Darab and P. A. Smith, "Chemistry of Technetium and Rhenium Species During Low-Level Radioactive Waste Vitrification," *Chem. Mater.*, 8 [5] 1004–1021 (1996).
4. T. May, K. S. Matlack, I. S. Muller, I. L. Pegg, and I. Joseph, Improved Technetium Retention in Hanford LAW Glass—Phase 1 Final Report, Washington River Protection SolutionsRPP-RPT-45887 (2010).
5. D. S. Kim, *et al.*, *Investigation of Tc Migration Mechanism During bulk Vitrification Process Using Re Surrogate*, Pacific Northwest National Laboratory, Richland, WA, PNNL-16267 (2006).

6. D. S. Kim, *et al.*, *Tc Reductant Chemistry and Crucible Melting Studies with Simulated Hanford Low-Activity Waste*, Pacific Northwest National Laboratory, Richland, WA, PNNL-15131 (2005).
7. J. M. MacKenzie and D. Canil, "Experimental Constraints on the Mobility of Rhenium in Silicate Liquids," *Geochim. Cosmochim. Acta*, 70 [20] 5236–5245 (2006).
8. H. Migge, "Thermochemical Comparison of the Systems Re–O and Tc–O," *Mat. Res. Soc. Symp. Proc.*, 127 205–213 (1989).
9. W. Ertel, H. S. C. O'Neill, P. J. Sylvester, D. B. Dingwell, and B. Spettel, "The Solubility of Rhenium in Silicate Melts: Implications for the Geochemical Properties of Rhenium at High Temperatures," *Geochim. Cosmochim. Acta*, 65 [13] 2161–2170 (2001).
10. A. C. Buechele, D. A. McKeown, W. W. Lukens, D. K. Shuh, and I. L. Pegg, "Tc and Re Behavior in Borosilicate Waste Glass Vapor Hydration Tests II," *J. Nucl. Mater.*, 429 [1–3] 159–165 (2012).
11. W. W. Lukens, D. A. McKeown, A. C. Buechele, I. S. Muller, D. K. Shuh, and I. L. Pegg, "Dissimilar Behavior of Technetium and Rhenium in Borosilicate Waste Glass as Determined by X-ray Absorption Spectroscopy," *Chem. Mater.*, 19 [3] 559–566 (2007).
12. ASTM International, "Standard Test Method for Measuring Waste Glass or Glass Ceramic Durability by Vapor Hydration Test (C 1663—09)," 2009.
13. D. A. McKeown, A. C. Buechele, W. W. Lukens, D. K. Shuh, and I. L. Pegg, "Tc and Re Behavior in Borosilicate Waste Glass Vapor Hydration Tests," *Environ. Sci. Technol.*, 41 [2] 431–436 (2006).
14. M. I. Ojovan, A. Pankov, and W. E. Lee, "The Ion Exchange Phase in Corrosion of Nuclear Waste Glasses," *J. Nucl. Mater.*, 358 [1] 57–68 (2006).
15. J. S. McCloy, *et al.*, "Rhenium Solubility in Borosilicate Nuclear Waste Glass: Implications for the Processing and Immobilization of Technetium-99," *Environ. Sci. Technol.*, (2012).
16. J. McCloy, *et al.*, *Rhenium Solubility in Borosilicate Nuclear Waste Glass: Implications for the Processing and Immobilization of Technetium-99*, Pacific Northwest National Laboratory, Richland, WA, PNNL-21553, Rev 0 (2012).
17. K. S. Matlack, I. Joseph, W. L. Gong, I. S. Muller, and I. L. Pegg, *Glass Formulation Development and DM10 Melter Testing with ORP LAW Glasses*, Vitreous State Laboratory, the Catholic University of America, Washington, DC, VSL-09R1510-2 (2009).
18. I. S. Muller, G. Diener, I. Joseph, and I. L. Pegg, *Proposed Approach for Development of LAW Glass Formulation Correlation*, Vitreous State Laboratory, the Catholic University of America, Washington, DC, VSL-04L44960-1, Rev 0 (2004).
19. W. W. Lukens, D. K. Shuh, I. S. Muller, and D. A. McKeon, "X-ray Absorption Fine Structure Studies of Speciation of Technetium in Borosilicate Glasses," *Mat. Res. Soc. Symp. Proc.*, 802 DD3.3.1–DD3.3.6 (2004).
20. D. S. Musselwhite and M. J. Drake, "Early Outgassing of Mars: Implications from Experimentally Determined Solubility of Iodine in Silicate Magmas," *Icarus*, 148 [1] 160–175 (2000).
21. D. S. Musselwhite, M. J. Drake, and T. D. Swindle, "Early Outgassing of Mars Supported by Differential Water Solubility of Iodine and Xenon," *Nature*, 352 [6337] 697–699 (1991).
22. K. E. Kelsey, J. R. Allwardt, and J. F. Stebbins, "Ca–Mg Mixing in Aluminosilicate Glasses: An Investigation Using ^{17}O MAS and 3QMAS and ^{27}Al MAS NMR," *J. Non-Cryst. Solids*, 354 [40–41] 4644–4653 (2008).
23. M. Edén, P. Sundberg, and C. Stålhandske, "The Split Network Analysis for Exploring Composition–Structure Correlations in Multi-Component Glasses: II. Multinuclear NMR Studies of Alumino-Borosilicates and Glass-Wool Fibers," *J. Non-Cryst. Solids*, 357 [6] 1587–1594 (2011).
24. E. Hellmut, "Structural Characterization of Noncrystalline Solids and Glasses Using Solid State NMR," *Prog. Nucl. Magn. Reson. Spectrosc.*, 24 [3] 159–293 (1992).
25. R. J. Kirkpatrick and R. K. Brow, "Nuclear Magnetic Resonance Investigation of the Structures of Phosphate and Phosphate-Containing Glasses: A Review," *Solid State Nucl. Magn. Reson.*, 5 [1] 9–21 (1995).
26. G. Engelhardt and D. Michel, *High Resolution Solid State NMR of the Silicates and Zeolites*. John Wiley & Sons, New York, 1987.
27. J. Murdoch, J. Stebbins, I. Carmichael, and A. Pines, "A Silicon-29 Nuclear Magnetic Resonance Study of Silicon-Aluminum Ordering in Leucite and Analcite," *Phys. Chem. Miner.*, 15 [4] 370–382 (1988).
28. A. Zazzi, *et al.*, "Structural Investigations of Natural and Synthetic Chlorite Minerals by X-Ray Diffraction, Mossbauer Spectroscopy and Solid-State Nuclear Magnetic Resonance," *Clays Clay Miner.*, 54 [2] 252–265 (2006).
29. S. K. Lee and J. F. Stebbins, "Al–O–Al and Si–O–Si Sites in Framework Aluminosilicate Glasses with Si/Al = 1: Quantification of Framework Disorder," *J. Non-Cryst. Solids*, 270 [1–3] 260–264 (2000).
30. L. van Wüllen, W. Müller-Warmuth, D. Papageorgiou, and H. J. Pentinghaus, "Characterization and Structural Developments of Gel-Derived Borosilicate Glasses: A Multinuclear MAS-NMR Study," *J. Non-Cryst. Solids*, 171 [1] 53–67 (1994).
31. S. V. Mattigod, B. Peter McGrail, D. E. McCready, L.-Q. Wang, K. E. Parker, and J. S. Young, "Synthesis and Structure of Perrhenate Sodalite," *Microporous Mesoporous Mater.*, 91 [1–3] 139–144 (2006).
32. P. J. Hendra, P. Le Barazer, and A. Crookell, "Fourier Transform Raman Spectra of Deeply Coloured Inorganic Species. I–The Permanganate Ion," *J. Raman Spectrosc.*, 20 [1] 35–40 (1989).
33. R. A. Johnson, M. T. Rogers, and G. E. Leroi, "Vibrational Spectra of Ammonium and Other Scheelite-Type Perrhenates," *J. Chem. Phys.*, 56 [2] 789–792 (1972).
34. R. P. Hapanowicz and R. A. Condrate Sr, "Raman Spectral Investigation of Sulfate Inclusions in Sodium Calcium Silicate Glasses," *J. Solid State Chem.*, 123 [1] 183–185 (1996).
35. M. Lenoir, A. Grandjean, S. Poissonnet, and D. R. Neuville, "Quantitation of Sulfate Solubility in Borosilicate Glasses Using Raman Spectroscopy," *J. Non-Cryst. Solids*, 355 [28–30] 1468–1473 (2009).
36. T. Tsujimura, X. Xue, M. Kanzaki, and M. J. Walter, "Sulfur Speciation and Network Structural Changes in Sodium Silicate Glasses: Constraints from NMR and Raman Spectroscopy," *Geochim. Cosmochim. Acta*, 68 [24] 5081–5101 (2004).
37. D. A. McKeown, I. S. Muller, H. Gan, I. L. Pegg, and C. A. Kendziora, "Raman Studies of Sulfur in Borosilicate Waste Glasses: Sulfate Environments," *J. Non-Cryst. Solids*, 288 [1–3] 191–199 (2001).
38. D. A. McKeown, A. C. Buechele, W. W. Lukens, D. K. Shuh, and I. L. Pegg, "Raman Studies of Technetium in Borosilicate Waste Glass," *Radiochim. Acta*, 95 [5] 275–280 (2007).
39. W. P. Griffith, "Infrared Spectra of Tetrahedral Oxyanions of the Transition Metals," *J. Chem. Soc., A*, 1467–1468 (1966).
40. R. K. Mishra, *et al.*, "Role of Sulfate in Structural Modifications of Sodium Barium Borosilicate Glasses Developed for Nuclear Waste Immobilization," *J. Am. Ceram. Soc.*, 91 [12] 3903–3907 (2008).
41. L. Backnaes and J. Deubener, "Experimental Studies on Sulfur Solubility in Silicate Melts at Near-Atmospheric Pressure," *Rev. Miner. Geochem.*, 73 143–165 (2011).
42. M. I. Ojovan and W. E. Lee, *An Introduction to Nuclear Waste Immobilisation*. Elsevier Science, Amsterdam, 2005.
43. B. J. Greer and S. Kroeker, "Characterisation of Heterogeneous Molybdate and Chromate Phase Assemblages in Model Nuclear Waste Glasses by Multinuclear Magnetic Resonance Spectroscopy," *Phys. Chem. Chem. Phys.*, 14 [20] 7375–7383 (2012).
44. F. A. Lifanov, M. I. Ojovan, S. V. Stefanovsky, and R. Burcel, "Feasibility and Experience to Vitrify NPP Operational Waste," *WM'03*, Tucson, AZ, February 23–27, 2003.
45. G. Calas, M. Le Grand, L. Galoisy, and D. Ghaleb, "Structural Role of Molybdenum in Nuclear Glasses: An EXAFS Study," *J. Nucl. Mater.*, 322 [1] 15–20 (2003).
46. D. Caurant, *et al.*, "Structural Investigations of Borosilicate Glasses Containing MoO_3 by MAS NMR and Raman Spectroscopies," *J. Nucl. Mater.*, 396 [1] 94–101 (2010).
47. D. Caurant, P. Loiseau, O. Majerus, V. Aubin-Chevaldonnet, I. Bardez, and A. Quintas, *Glasses, Glass–Ceramics and Ceramics for Immobilization of Highly Radioactive Nuclear Wastes*. Nova Science Publishers, Inc., New York, 2009.